JOURNAL OF MAGNETIC RESONANCE **129,** 105–108 (1997)
ARTICLE NO. MN971253

Nuclear Magnetic Resonance Imaging of Solid Rocket Propellants at 14.1 T

W. E. Maas,* L. H. Merwin,† and D. G. Cory‡

*Bruker Analytical Systems, Inc., 19 Fortune Drive, Billerica, Massachusetts 01821; †Chemistry and Materials Branch, Weapons Division, Naval Air Warfare Center, China Lake, California 93555; and ‡Department of Nuclear Engineering, NW14-4111, Massachusetts Institute of Technology, 150 Albany Street, Cambridge, Massachusetts 02139

Received April 24, 1997; revised July 18, 1997

Proton NMR images of solid propellant materials, consisting of a polybutadiene binder material filled with 82% solid particles, have been obtained at a magnetic field strength of 14.1 T and at a resolution of 8.5 × 8.5 μm. The images are the first of elastomeric materials obtained at a proton frequency of 600 MHz and have the highest spatial resolution yet reported. The images display a high contrast and are rich in information content. They reveal the distribution of individual filler particles in the polymer matrix as well as a thin polymer film of about 10–30 μm which is found to surround some of the larger filler particles.

Solid rocket motor propellants generally consist of an elastomeric binder material highly filled with particulate oxidizer (*1*). Important characteristics such as burn rate and mechanical properties are affected by the distribution and concentration of the filler particles and the properties of the polymer matrix. Ideally the filler is uniformly distributed and the matrix is free of voids. Nuclear magnetic resonance (NMR) imaging has been shown to be a useful tool for obtaining physical and chemical information of elastomeric samples (*2–4*) and of propellant materials (*5, 6*). Here we describe proton NMR images at a magnetic field strength of 14.1 T (corresponding with a proton frequency of 600 MHz). These images have an in-plane resolution of 8.5 × 8.5 μm and are the first NMR imaging data of elastomeric materials obtained at 600 MHz and the first at such a high spatial resolution. The enhanced sensitivity and resolution available at this high field strength is crucial to obtaining a complete picture of the propellant characteristics since the length scale of the small filler particles in the material is below the spatial resolution normally achieved.

NMR imaging of materials is typically performed at field strengths of 3 to 10 T. An example of such an image of a propellant is shown in Fig. 1, obtained at a magnetic field strength of 3 T and with an in-plane resolution of 35 × 35 μm. The image displays the proton density of the binder material and the areas of low intensity in this image show the spatial distribution of the filler particles. Although the image resolution is high enough to detect features such as particle distribution and voids, it is insufficient to study details such as the spatial distribution of small (<35 μm) particles and small-scale intensity fluctuations.

A difficulty in increasing the image resolution is that this naturally decreases the volume of the voxel and hence the number of spins per voxel. All else being equal this would lead to a decrease in the signal-to-noise ratio of the image. This loss can be overcome by performing the imaging experiments at a higher magnetic field strength since the sensitivity of the NMR experiment scales with the field strength to the power 7/4. In this case the approximately 40-fold decrease in voxel volume has been compensated by a nearly 5-fold increase in field strength and a higher efficiency detection circuit. In addition to the sensitivity advantages at higher fields, there is also a potential increase in contrast due to susceptibility differences, which scale with the field strength.

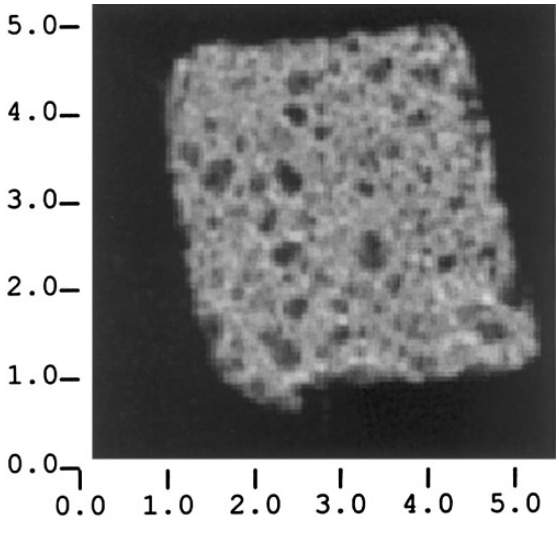

FIG. 1. A single plane from a 3D proton spin echo image of a propellant material. The image is obtained at 3 T with an in-plane resolution of 35 × 35 μm and a plane thickness of 120 μm. The image displays the proton density of the propellant, due to the binder material. The large and small voids are due to the filler particles.

1090-7807/97 $25.00

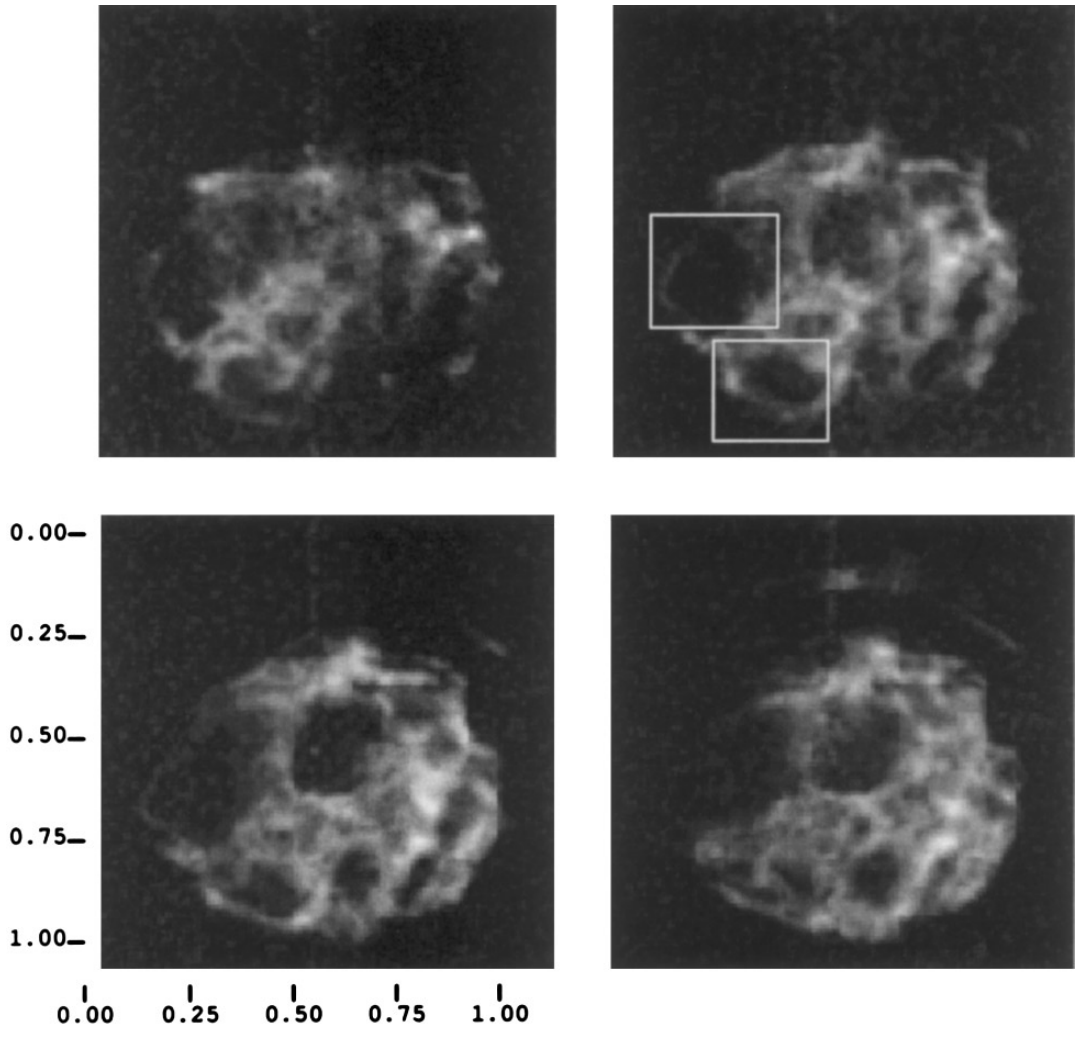

FIG. 2. Four subsequent planes from a 3D image of a HTPB-based propellant, obtained at 14.1 T. The in-plane resolution is 9×9 μm and the thickness per plane is 45 μm. The sample was contained in a 1-mm-o.d. glass tube. The voids are due to the ammonium sulfate filler particles of varying size. The rectangles in the upper right image indicate the expanded areas shown in Fig. 4. The 3D image was acquired with $128 \times 128 \times 16$ data points, an echo time of 1 ms, a repetition time of 1 s, and a phase encoding time of 0.5 ms, and the total experiment time was 10 h. A gradient strength of 2.5 T/m and a receiver bandwidth of 125 kHz were used.

Since the number of pixels one can obtain across an imaged plane is constant and limited by the proton transverse relaxation time T_2 (*7, 8*), an increase in image resolution for a constant sample size would result in a proportionally larger receiver bandwidth and therefore an increase in noise, which can be avoided by decreasing the field of view. The NMR images in Figs. 2, 3, and 4 are obtained on a 14.1-T system, with a vertical bore magnet that has a room temperature bore of 54 mm. This system is based on a Bruker AMX console. The NMR imaging experiments are obtained with a special RF probe for microscopy studies (*9*) capable of image resolutions as fine as 2 μm. The RF probe employs a 1-mm sample coil, tightly wound around the sample, resulting in a high filling factor which leads to an increased S/N and further offsets the losses in sensitivity from going to a higher image resolution. The gradient set is capable of generating 1000 G/cm in two directions and 300 G/cm along the coil axis.

The rocket motor propellant materials studied here are inert materials in which ammonium sulfate replaces the oxidizer ammonium perchlorate. The solids loading of the sample is 82% by weight and consists either entirely of ammonium sulfate or of ammonium sulfate and aluminum powder. The ammonium sulfate crystals have a bimodal distribution, consisting of crystals with an average size of 200 μm, and crystals with an average size of 20 μm, while the aluminum particles are approximately 5 μm in size. The binder material is hydroxy-terminated poly butadiene (HTPB) (5% by weight), which is cured with isopherone diisocyanate and plasticized with dioctyl phthalate (12% by weight).

The NMR images are obtained with three-dimensional spin echo gradient sequences. Spin echo sequences have

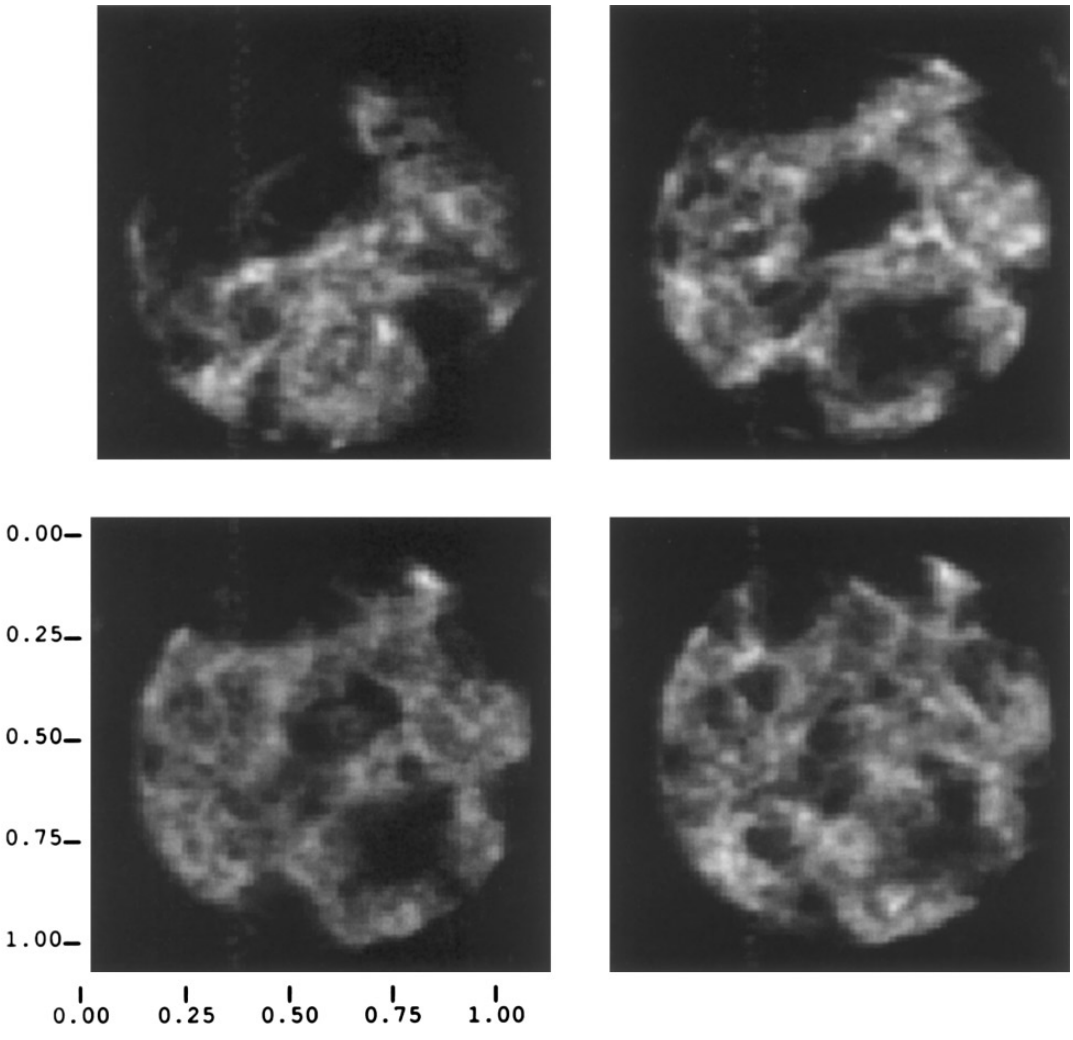

FIG. 3. Four subsequent planes from a 3D image of similar HTPB-based propellant, which in addition to ammonium sulfate contains aluminum filler particles. The images were obtained at 14.1 T. The in-plane resolution is 8.3 × 8.3 μm and the plane thickness is 45 μm. The experimental conditions are similar to those listed in the legend to Fig. 2.

a good signal-to-noise since their relaxation properties are determined by the true transverse relaxation time T_2 and these methods record a truer measure of the proton spin density than do gradient echo methods. In the propellant images we observe the spatial distribution of the binder material, i.e., the protons of HTPB and those of the plasticizer. A single transverse relaxation time T_2 of 8 ms is observed for these protons. The protons present in the ammonium sulfate filler have a much shorter T_2 and are not observed.

The 3-T NMR image in Fig. 1 is typical for HTPB-based propellant materials and displays the proton density of the material. The large and small voids are caused by the ammonium sulfate filler particles, which are present in a bimodal distribution. Some of the larger voids are partially surrounded by a higher intensity rim. These rims are not caused by susceptibility artifacts, since they are observed in both the read and the phase encoding directions, and they indicate an increased proton density adjacent to the filler particles. Some pronounced susceptibility artifacts have been observed in different samples for which we have yet to identify the origin. In addition it seems that the image reveals a small-scale roughly periodic fluctuation of the proton density as well as bright spots. In order to examine these findings in more detail the samples were reexamined at a resolution of 8.5 × 8.5 × 45 μm.

Figures 2 and 3 show some representative planes from three-dimensional images of HTPB-based propellants. The samples are contained in 1-mm-o.d. glass tubes and the experimental parameters are given in the figure legends. The fact that not all of the images appear round is due to large filler particles at the edges of the sample. The propellant samples imaged in Figs. 2 and 3 are similar, but for the addition of aluminum powder (6.5%) to the latter sample. These aluminum particles have a size of about 5 μm and are therefore not individually resolved in the images.

The images clearly display the large filler particles in

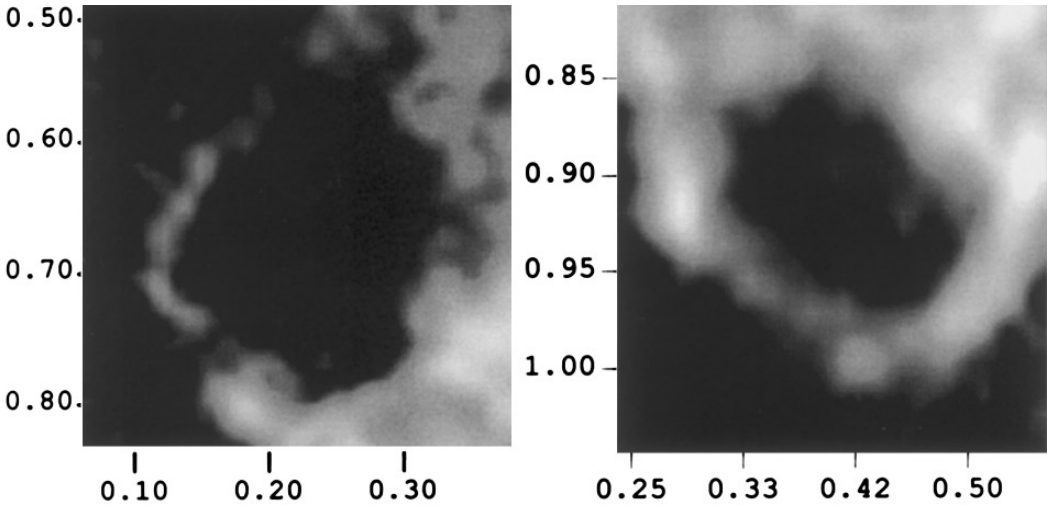

FIG. 4. Two expansions from the upper right image in Fig. 2. The images are subsets of the original data and smoothed with a bilinear interpolation method using the visualization program Transform (*10*). The expansions display the thin polymer film surrounding two of the larger filler particles found in the lower left corner of the original image.

addition to individual ammonium sulfate crystals as small as 20 μm. Apart from these obvious features, the images are characterized by a very heterogeneous density distribution in between the filler particles with intensities ranging from near zero to approximately three times the nominal intensity, revealed in the images as bright spots. This heterogeneity may be caused by differences in the chemical composition of the binder material (resulting in different transverse relaxation times), by traces of unfilled binder material, or by an uneven distribution of the small filler particles in combination with an averaging of the proton intensities over the thickness of the imaged planes. Images obtained from a sample of unfilled HTPB, however, display a very homogeneous density distribution and a preliminary conclusion is that the heterogeneities observed in the propellant images is most likely due to the distribution of small filler particles.

A potentially important phenomenon observed in the 125-MHz proton images is the appearance of a higher intensity rim around the larger filler particles. This is examined in detail in the 600-MHz images. Figure 4 shows two expansions from the upper right image of Fig. 2. The images, obtained by expanding and smoothing the original data, display the immediate surroundings of two filler particles found in the lower left corner of the original image. The expansions reveal a thin polymer film of about 10–30 μm, surrounding the filler particles. The film closely follows the contour of the filler particle and most likely is caused by adhesion to the ammonium sulfate crystal.

These 600-MHz proton images display a high information content and show that imaging at such high field strengths is both feasible and useful for the study of heterogeneous materials in general and solid fuel propellant samples in particular. Through a quantitative study of the morphology of these complex materials it may be possible to correlate the microscopic composition to the physical properties of the propellants.

ACKNOWLEDGMENTS

The authors thank Xiao Wu Tang for support in obtaining the images at 14.1 T and Drs. Tom Stephens and Tony Wallner for the preparation of the propellant samples. This work was funded in part by the Department of Defense (SBIR N68936-96-C-0178), the National Science Foundation (DMR-9357603), and the National Institute of Health (ROI-GM52026, RR-00995).

REFERENCES

1. G. P. Sutton, ''Rocket Propulsion Elements: An introduction to the Engineering of Rockets,'' 6th ed., Wiley, New York (1992).
2. M. A. Rana and J. L. Koenig, *Macromolecules* **27,** 3727 (1994).
3. W. Kuhn, P. Barth, P. Denner, and R. Muller, *Solid State NMR* **6,** 295 (1996).
4. P. Blumler and B. Blumich, *in* ''NMR—Basic Principles and Progress (P. Diehl, E. Fluck, and R. Kosfeld, Eds.), Vol. 30, Springer-Verlag, Berlin/New York (1993).
5. L. H. Merwin, R. A. Nissan, T. S. Stephens, and A. S. Wallner, *J. Appl. Polym. Sci.* **62,** 341 (1996).
6. S. W. Sinton, J. H., Iwamiya, B. Ewing, and G. P. Drobny, *Spectroscopy* **6,** 42 (1991).
7. D. G. Cory and W. S. Veeman, *J. Magn. Reson.* **84,** 392 (1989).
8. D. G. Cory, A. N. Garroway, and J. B. Miller, *J. Magn. Reson.* **87,** 202 (1990).
9. S. M. Choi, X. Tang, and D. G. Cory, *Int. J. Imaging Syst. Technol.* **8,** 263 (1997).
10. Fortner Research LLC, Sterling, VA.